Development 138, 4911-4919 (2011) doi:10.1242/dev.068122

Complex functions of *Mef2* splice variants in the differentiation of endoderm and of a neuronal cell type in a sea anemone

Grigory Genikhovich and Ulrich Technau*

SUMMARY

In triploblastic animals, mesoderm gives rise to many tissues and organs, including muscle. By contrast, the representatives of the diploblastic phylum Cnidaria (corals, sea anemones, jellyfish and hydroids) lack mesoderm but possess muscle. In vertebrates and insects, the transcription factor Mef2 plays a pivotal role in muscle differentiation; however, it is also an important regulator of neuron differentiation and survival. In the sea anemone *Nematostella vectensis*, an organism that lacks mesoderm but has muscles and neurons, *Mef2* (*Nvmef2*) has been reported in single ectodermal cells of likely neural origin. To our surprise, we found that *Nvmef2* is alternatively spliced, forming differentially expressed variants. Using morpholino-mediated knockdown and mRNA injection, we demonstrate that specific splice variants of *Nvmef2* are required for the proliferation and differentiation of endodermal cells and for the development of ectodermal nematocytes, a neuronal cell type. Moreover, we identified a small conserved motif in the transactivation domain that is crucially involved in the endodermal function of Nvmef2. The identification of a crucial and conserved motif in the transactivation domain predicts a similarly important role in vertebrate Mef2 function. This is the first functional study of a determinant of several mesodermal derivatives in a diploblastic animal. Our data suggest that the involvement of alternative splice variants of *Mef2* in endomesoderm and neuron differentiation predates the cnidarian-bilaterian split.

KEY WORDS: Mef2, Endoderm development, *Nematostella*

INTRODUCTION

Among the fundamental questions in biology is the evolutionary origin of the nervous system and the musculature in multicellular animals. The differentiation of these key tissues is governed by a set of conserved transcription factors. Many of these transcription factors have diverse functions in the development of several tissues and developmental processes. Identifying the ancestral role of these transcription factors would be a crucial step in reconstructing the evolution of the tissues involved. One of the key determinants of both muscle and neuronal development in vertebrates and flies is the transcription factor myocyte enhancer factor 2 (Mef2) (Potthoff and Olson, 2007). Although the highest expression levels of *Mef2* are in muscle and neuronal tissue (Black et al., 1997), in vertebrates it is also expressed in some other tissues. It has been reported that mouse *Mef2* is expressed ubiquitously at low levels (Yu et al., 1992). In combination with Twist, Mef2 is one of the key regulators of muscle differentiation in flies (Sandmann et al., 2007; Sandmann et al., 2006) and vertebrates (Wang et al., 2001), where it also regulates cartilage and bone formation from the mesodermal and neural crest precursor cells (Arnold et al., 2007; Verzi et al., 2007). In addition, in vertebrates, Mef2 plays an important role in neuron and lymphocyte differentiation and survival/apoptosis (Ananieva et al., 2008; Wang et al., 2009), as well as in activity-dependent synapse formation (Flavell et al., 2006; Flavell et al., 2008). Neuronal expression of *Mef2* and its role in circadian behaviour have also been shown in insects (Blanchard et al., 2010; Farris et al., 1999; Schulz et al., 1996). Whereas invertebrates possess a single *Mef2* gene, vertebrates possess four paralogues, termed *Mef2a*, *Mef2b*, *Mef2c* and *Mef2d*, which are expressed in overlapping, but distinct, domains (Potthoff and Olson, 2007).

Mef2 binds DNA with its conserved N-terminal MADS domain. The MADS domain is directly followed by a short conserved Mef2 domain. Together, they facilitate DNA binding, dimerisation and co-factor recruitment. The C-terminal transactivation domain shows very little conservation, even between the four vertebrate Mef2 paralogues (Potthoff and Olson, 2007). In both protostomes and deuterostomes, *Mef2* mRNA is alternatively spliced to produce multiple isoforms, which, in part, are differentially expressed (Martin et al., 1994; Gunthorpe et al., 1999; Zhu and Gulick, 2004; Zhu et al., 2005). Little is known about the specific functions of these splice variants in Bilateria. A recent report suggests that aberrant splice variants are involved in myogenic disorders (Bachinski et al., 2010). It is unclear what the ancestral function of *Mef2* was and whether alternative splicing of *Mef2* arose independently in vertebrates and invertebrates.

In this context, investigating the role of *Mef2* in cnidarians is of particular importance. These diploblastic organisms are among the earliest diverging animal groups to possess a nervous system and muscles. A cnidarian *Mef2* homologue (*PcMef2*) was first reported in the hydrozoan *Podocoryne carnea* (Spring et al., 2002). *PcMef2* expression is upregulated in the larval endoderm and the endoderm of the polyp at the site of the medusa bud. *PcMef2* is also expressed in the plate endoderm, the forming velum, the striated muscle and the tentacle buds of the forming medusa (Spring et al., 2002). Strikingly, in the sea anemone *Nematostella vectensis*, *Mef2* (*Nvmef2*) was described as an ectodermally expressed gene (Martindale et al., 2004). The transcript was detected in single cells throughout embryonic and larval development (Martindale et al., 2004). These cells are

Department for Molecular Evolution and Development, Centre of Organismal Systems Biology, University of Vienna, Althanstraße 14, A-1090 Vienna, Austria.

*Author for correspondence (ulrich.technau@univie.ac.at)

Accepted 9 September 2011

likely to be precursors of neurons or the cnidarian-specific nematocytes. Nematocytes are sensory stinging cells that are considered to be a neuronal cell type (Watanabe et al., 2009).

To gain further insight into the function of cnidarian *Mef2*, we performed a detailed analysis of this gene in *N. vectensis*. We identified six alternative splice variants of *Nvmef2* that fall into two groups with respect to protein structure and expression pattern. Antisense morpholino knockdown experiments demonstrated that one group of *Nvmef2* splice variants is crucial for proper endoderm development. Our data suggest that the dual role of Mef2 proteins in neural and non-neural tissue differentiation predated the cnidarian-bilaterian split.

MATERIALS AND METHODS

Animal culture

Animals were cultured and spawning was induced as described (Fritzenwanker and Technau, 2002; Genikhovich and Technau, 2009a).

Cloning and expression analysis

The *Nvmef2* splice variants were cloned by PCR based on the EST and genomic sequences. Accession numbers for splice variants I to VI are: HQ634794, HQ634795, HQ634796, HQ634797, HQ634798 and HQ634799, respectively. In situ hybridisation was performed as described (Genikhovich and Technau, 2009b). The *NvNcol3* probe was generated based on GenBank sequence FC288770. RT-PCR analysis of cDNA samples was normalised to β-*actin*. For β-*actin* and *Nvmef2*, 21 and 32 PCR cycles were used, respectively.

Morpholino (MO) experiments and plasmid injection

The activity and specificity of the *Nvmef2* translation-blocking MO (ATG-MO) was confirmed in vitro (TnT Quick Coupled Transcription/Translation System, Promega). The mRNA transcribed from the plasmid carrying six silent mutations (AUGGGGCGAAAGAAGAUCCAGAUAU to AUGGGCAGGAAAAAGAUUCAAAUAU) was not recognised by the ATG-MO, whereas translation from the wild-type mRNA was suppressed in a concentration-dependent manner (supplementary material Fig. S1). The sequences (5′ to 3′) and working concentrations of the microinjected MOs are: ATG-MO, ATATCTGGATCTTCTTTCGCCCCAT, 125 μM; MOex9, GATGTGCCTAGGGTACAACAACAAT, 500 μM; MOex10, GAAGTCTATGGAGATGATACAGGTA, 500 μM; and MOint10, ACCAATAAGAAAGTTCCTTACCCCT, 125 μM.

For rescue experiments, 125 μM MOex9 or MOint10 containing 50 ng/μl *Nvmef2-IIwt* or *Nvmef2-IIΔC2* mRNA was injected into *Nematostella* zygotes and the embryos were allowed to develop for 6 days. The C2 box deletion in *Nvmef2-IIΔC2* was generated by PCR template switching using: Mef2E10_swF, GCAAACAGACACCCTCGATAACTTCCATCTAG-ACAG; and Mef2E10_swR, CTGTCTAGATGGAAGTTATCGAGGG-TGTCTGTTTGC.

The protein coding sequences of *Nvmef2-IIwt* and *Nvmef2-IIΔC2* were directionally cloned into pNvT (Renfer et al., 2010) digested with *Pac*I and *Sbf*I. mRNA synthesis was performed on a template produced by PCR using the mMessage mMachine SP6 Kit (Ambion).

For construction of the *MyHCΔMef::mCherry* vector, the two Mef2 and one SQUA/Agamous binding sites predicted with CONSITE (Lenhard et al., 2003) (score >9.5) in the *MyHC1* promoter sequence used by Renfer et al. (Renfer et al., 2010) were replaced by the following sequences: CTATAAAAAA (position 193) was changed to GGACGGGGGG; CTAAAAATAT (position 298) was changed to GGACGGGGGG; and CCAAATTTAGACAC (position 348) was replaced by GGCGGGGGTTGGCC. I-*Sce*I digestion and microinjection were performed as described (Renfer et al. 2010).

Phalloidin staining, DNA replication assay, TUNEL assay, histology and electron microscopy

Phalloidin and TO-PRO3 staining were performed as described (Genikhovich and Technau, 2009c). DNA replication was assayed with the Click-iT EdU Alexa Fluor 488 Imaging Kit (Invitrogen). EdU pulses of 25 minutes were used to label the nuclei. The S-phase index was calculated from the percentage of nuclei incorporating EdU among all nuclei per confocal section. A single medial confocal section was counted for each embryo. Nuclei from 8-16 confocal sections were counted for each datum point. The counts from embryos with the highest and lowest S-phase index in the endoderm were removed from the analysis. Imaging was performed with a Leica SP2 confocal microscope. TUNEL staining on 16 μm cryosections was performed with the In Situ Cell Death Detection Kit, Fluorescein (Roche). Transmission electron microscopy and semi-thin sectioning were performed according to standard techniques (Fritzenwanker et al., 2007).

RESULTS

Characterisation of *Nvmef2* alternative splice variants

In order to gain insight into the ancestral structure of Mef2, we searched an EST dataset from the sea anemone *Nematostella vectensis* (Technau et al., 2005) for the presence of a *Mef2* homologue. We identified a cDNA homologous to *Mef2*, which only partly matched the published sequence of *Nematostella Mef2* (*Nvmef2*) (Martindale et al., 2004). This suggested that *Nvmef2* is differentially spliced. Based on the alignment of the different *Nvmef2* ESTs and the published *Nvmef2* mRNA sequence with the genomic sequence on scaffold 140 as well as on PCR analysis, we conclude that *Nvmef2* contains at least 11 exons (Fig. 1A). We confirmed six alternative splice variants by PCR (Fig. 1B). All splice variants share the conserved MADS and Mef2 domains as well as a conserved stretch of sequence directly downstream of the Mef2 domain. However, the splice variants differ drastically in the sequence encoding the C-terminal region of the protein and in the 3′ UTRs. Two classes can be distinguished: (1) splice variants I and II containing exons 9-11 (*Nvmef2-I* and *Nvmef2-II*); and (2) splice variants III-VI containing exon 7 (*Nvmef2-III*, *-IV*, *-V* and *-VI*) (Fig. 1B). Exon-intron boundaries are conserved between *Nematostella*, vertebrates, amphioxus and *Drosophila* in the two exons encoding the MADS box and the Mef2 domain. The sequence outside of these domains is too divergent to make any confident predictions about the conservation of the exon-intron structure between *Nvmef2* and bilaterian *Mef2*.

The transcripts containing exon 7 differ due to the alternative splice acceptor sites in exon 7 (Fig. 1A,B). *Nvmef2-IV* represents the published sequence (Martindale et al., 2004). Whereas the exon 9-containing *Nvmef2-I* and *Nvmef2-II* encode predicted Mef2 proteins of ‘conventional’ size (>450 amino acids), comparable to bilaterian Mef2 (Fig. 1C), the putative proteins encoded by the exon 7-containing splice variants are significantly shorter, with exon 7 encoding only 33, 5, 9 and 8 amino acids in splice variants III-VI, respectively, followed by long 3′ UTRs of up to 1758 bp.

Alignment of the deduced Nvmef2 protein sequence with Mef2 proteins of other species shows 96-100% amino acid similarity for both the MADS and Mef2 domains within Eumetazoa (Fig. 1C; supplementary material Fig. S2A). The transactivation domain following the Mef2 domain in the eumetazoan proteins can be subdivided into four regions (Fig. 1C). The first region (41 amino acids in *Nematostella*, which we termed C1) directly following the Mef2 domain is 75% similar to the corresponding C1 domain in bilaterian Mef2 proteins (Fig. 1C; supplementary material Fig. S2A). C1 contains the sequence homologous to the muscle-specific variant of the so-called α-domain located in the alternatively spliced coding exon 3α2 in vertebrates [exon 1b according to Martin et al. (Martin et al., 1994)]. Interestingly, we did not find a splice variant that includes the sequence corresponding to the

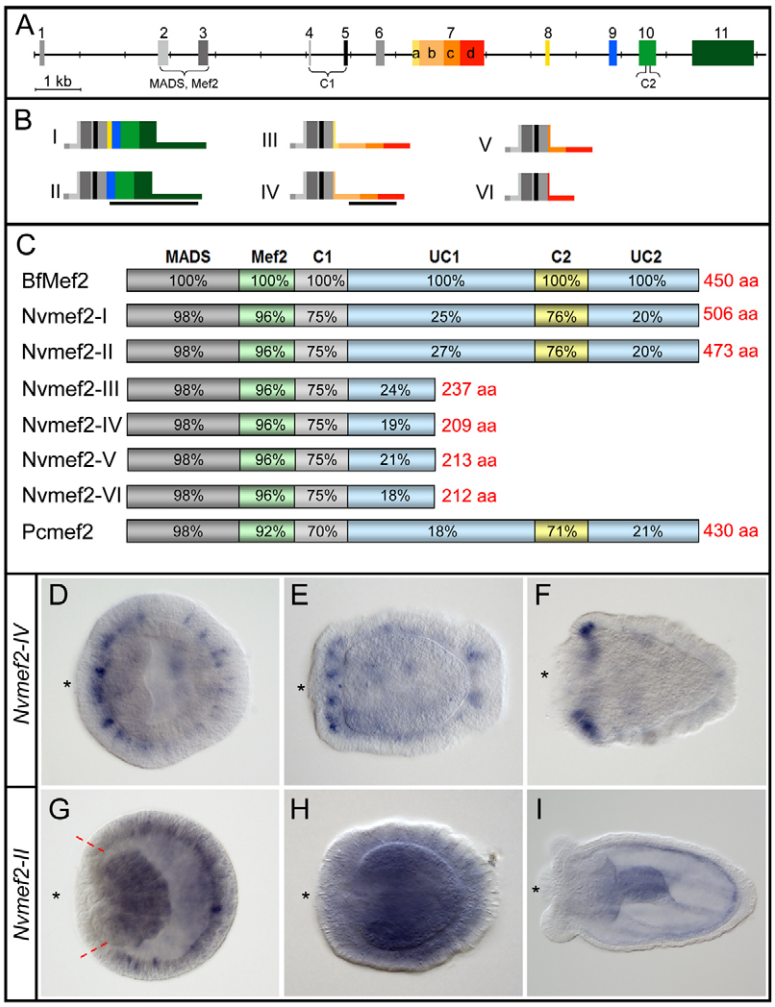

Fig. 1. Genomic structure and expression of *Nvmef2*. (**A**) Exon-intron structure of *Nvmef2*. (**B**) Six alternative splice variants of *Nvmef2* were confirmed by PCR, cloning and sequencing. The colour coding and scale of the exons is the same as in A. Regions flanking the exon boxes represent UTRs. Black bars beneath splice variants II and IV represent the in situ probes used for the hybridisation shown in D-I. (**C**) Amino acid (aa) conservation in different domains of cnidarian Mef2 proteins compared with the predicted BfMef2 from amphioxus (XP_002609948). Nvmef2-I, -II, -III, -IV, -V and -VI are six putative *Nematostella* Mef2 proteins encoded by the alternative splice variants. Pcmef2, *Podocoryne carnea* Mef2 (CAD21522). MADS, MADS domain; Mef2, Mef2 domain; C1, conserved region 1; UC1, unconserved region 1; C2, conserved region 2; UC2, unconserved region 2. (**D-F**) Ectodermal expression of *Nvmef2-IV* in single cells of (D) 2-day-old planula, (E) 4-day-old planula and (F) 6-day-old planula starting metamorphosis. (**G-I**) Expression of *Nvmef2-II* in (G) 24-hour-old gastrula, (H) 4-day-old planula and (I) 6-day-old primary polyp. At 24 hours, *Nvmef2-II* expression is stronger in the endoderm and in single ectodermal cells; the area of the ectoderm around the blastopore (between the red lines) is free of the transcript. Asterisks indicate mouth position.

vertebrate 3α1 variant, nor could we find the homologous sequence in the genomic sequence of *Nvmef2*. Also, unlike in vertebrates, the Nvmef2 α-domain is split between two exons, neither of which appears to be alternatively spliced. The C1 domain is followed by a large region that shows very little sequence similarity, and which in Nvmef2-I and Nvmef2-II is interrupted by a 44 amino acid serine and threonine-rich motif that we termed C2 (Fig. 1C). C2 shows relatively high evolutionary conservation (76% similarity over 44 amino acids between *Nematostella* and the corresponding amphioxus protein sequence; supplementary material Fig. S2B). This motif is more derived in the Protostomia Mef2, both in Ecdysozoa and Lophotrochozoa proteins, and is absent from vertebrate Mef2B, which appears to be the most derived vertebrate paralogue. In *Nematostella*, the conserved C2 box is encoded by the central part of *Nvmef2* exon 10. The so-called β- and γ-domains, which are known to be important regulatory modules in the transactivation domain of the mammalian Mef2 proteins and are encoded by alternatively spliced exons (Zhu and Gulick, 2004; Zhu et al., 2005; Hakim et al., 2010), do not align with the Nvmef2 sequence.

Nvmef2 splice variants show differential spatiotemporal expression

In situ hybridisation confirmed that the exon 7-containing splice variants are expressed in a subset of ectodermal cells (Fig. 1D-F), which have been interpreted as putative neuronal or nematocyte precursor cells (Martindale et al., 2004). The number of cells expressing exon 7-containing splice variants increases from the gastrula stage toward the mid-planula and then decreases. During metamorphosis (days 5-7), the expression of the exon 7-containing splice variants diminishes in the body column and localises in the tips of the emerging tentacles (Fig. 1D-F). In line with this, RT-PCR analysis showed very low levels of these splice variants at early and late stages of development, with a peak in expression in the gastrula and planula (supplementary material Fig. S3).

By contrast, RT-PCR showed that *Nvmef2-II* is a weakly expressed maternal transcript, and its levels are maintained throughout development, whereas *Nvmef2-I* is even weaker and only detectable from blastula to mid-planula stage (supplementary material Fig. S3). In situ hybridisation revealed that *Nvmef2-I* and *Nvmef2-II* expression is upregulated in the endoderm of the gastrulae, planulae and primary polyps, but also shows a slightly weaker expression in the ectoderm (Fig. 1G-I). An upregulation of expression was also observed in the individual ectodermal cells of the gastrula. This short-term increase in expression was, however, over by the planula stage. The area immediately around the blastopore of the gastrula, which gives rise to the future pharynx, was free of *Nvmef2-I* and *Nvmef2-II* expression.

Although specific sequences for some individual splice variants were too short to allow preparation of specific probes, we can state that the two classes of splice variants occupy distinct, albeit possibly overlapping, spatiotemporal expression domains.

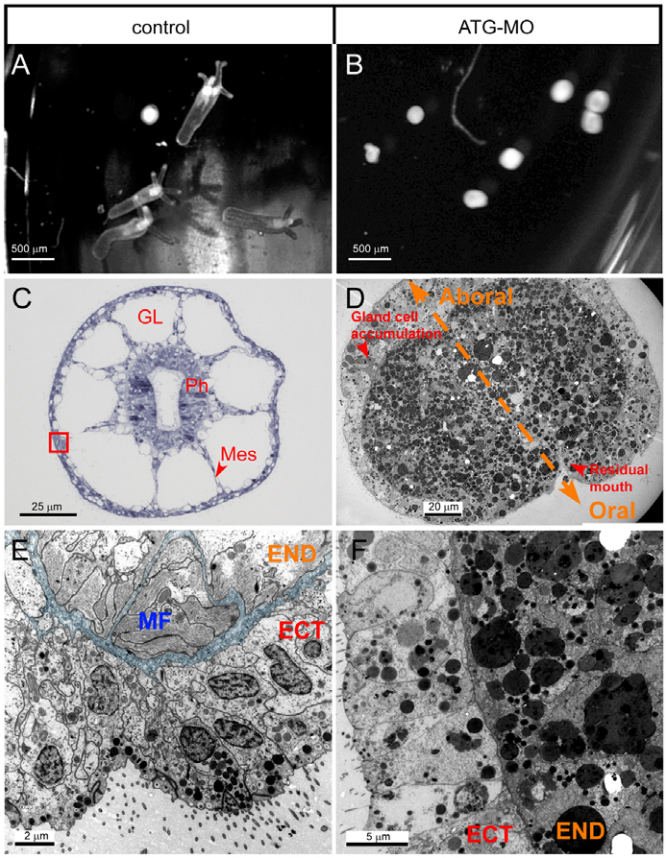

Fig. 2. Effects of ATG-MO on *Nematostella* embryo development. (**A**,**B**) Live image of (A) the control primary polyp and (B) the ATG-MO morphant (B). (**C**) Semi-thin section across the pharyngeal region of the primary polyp. The gut lumen (GL), which is subdivided into eight chambers by the mesenteries (Mes), and the pharynx (Ph) are visible. The boxed region corresponds approximately to the area shown in E. (**D**) Transmission electron microscopy of the ATG-MO morphant. The endoderm is scrambled and no gut lumen is visible. The oral-aboral axis and the underdeveloped pharynx are marked. (**E**,**F**) Fragments of the control primary polyp in the area of parietal muscle (E) and of the morphant embryo (F) at high magnification. In the morphant, the mesogloea is thin and the endodermal cells are undifferentiated and packed with electron-dense compound granules. No muscle fibres are visible. In the control, the endodermal cells are differentiated and muscle fibres are visible at the base of the endodermal cells. The mesogloea is thick (highlighted blue). ECT, ectoderm; END, endoderm; MF, muscle fibres. All morphants and controls are 8 days old.

Morpholino-mediated knockdown of Nvmef2 affects *N. vectensis* development

To gain insight into the function of *Nvmef2*, we performed antisense MO-mediated knockdown of *Nvmef2* translation. Microinjection of the translation-blocking MO (ATG-MO), which affects all splice variants, into *Nematostella* zygotes strongly affected development. Whereas 88% of the mock-injected embryos (n=105) developed into primary polyps by day 8, most (89%) of the embryos injected with ATG-MO (n=225) did not survive until day 8, and out of those that did (n=28), none underwent metamorphosis (Fig. 2A-D). Transmission electron microscopy (TEM) analysis of 8-day-old morphant embryos showed that they had an ectodermal layer with the normal epithelial and gland cells (supplementary material Fig. S4C,D), but the endoderm was scrambled and no gut lumen was visible (Fig. 2D). The gastric cavity was filled with loose cells packed with electron-dense granules (Fig. 2D,F). The mesogloea appeared to be much thinner than normal. The oral-aboral axis of the morphant embryo, however, appeared intact. The oral side was visible by a residual mouth opening (the former blastopore), and at the aboral side we found typical accumulations of the ectodermal gland cells (Fig. 2D), which are normally observed in the vicinity of the apical organ. Directional swimming of the morphant planulae was not perturbed. These morphants never developed further and died by day 12-14.

One of the hallmarks of endoderm differentiation in *Nematostella* is the formation of the mesenterial muscles. No muscle fibres could be observed by TEM in the morphants, in contrast to the mock-injected control primary polyps of the same age (Fig. 2E,F; supplementary material Fig. S4I for high magnification). Also, the expression of the retractor muscle-specific *Myosin heavy chain 1* (*MyHC1*) (Renfer et al., 2010) was not detectable in the 5-day-old morphant (supplementary material Fig. S5). Thus, the ATG-MO impairs endoderm differentiation and prevents further development and metamorphosis.

Exons 10 and 11 are required for normal function of Mef2 in the endoderm

To investigate the endodermal function of *Nvmef2* we focused on the endodermally expressed splice variants. We prevented proper splicing of exons 9, 10 and 11 by microinjecting zygotes with MOs designed against the splice acceptor site of exon 9 (MOex9), the splice acceptor site of exon 10 (MOex10), and the splice donor site at the 3′ end of exon 10 (MOint10).

Upon injection of MOex9, exon 9 is spliced out together with intron 8. The resulting mRNA has exon 10 in the correct reading frame, i.e. the Nvmef2 protein is missing the domain encoded by exon 9 but is otherwise intact (Fig. 3A). Although we demonstrated by RT-PCR that MOex9 causes mis-splicing of *Nvmef2* mRNA, the microinjected embryos developed normally into primary polyps (Fig. 3A). In contrast to MOex9, microinjection of MOex10 caused a strong phenotype. This MO links exon 9 to exon 11 in the incorrect reading frame, generating a stop codon shortly after the beginning of exon 11 (Fig. 3B). The morphant embryos displayed aberrations of endoderm development but proper oral-aboral axis patterning (Fig. 3B; supplementary material Fig. S4A,B). Hence, the loss of exon 9 (82 amino acids) has no phenotypic effect, whereas truncation of the last two exons (187 amino acids) is sufficient to phenocopy the endodermal phenotype of the ATG-MO. Microinjection of MOint10 caused incorporation of an intron 10 with several stop codons into the *Nvmef2* mRNA prior to exon 11. The predicted protein of this mis-spliced mRNA lacks 89 amino acids encoded by exon 11. Morphologically, the MOint10 and MOex10 morphants were indistinguishable (Fig. 3C). Since three independent MOs (ATG-MO, MOex10 and MOint10) all resulted in very similar and strong phenotypes, we conclude that the part of the protein encoded by exon 11 is essential for the role of Nvmef2 in endoderm development. This effect does not seem to rely simply on the shortening of the protein by 89 amino acids, as the removal of exon 9 (which encodes 82 amino acids) has no effect.

The conserved C2 motif is encoded by a sequence located not in exon 11, but in exon 10. To elucidate the function of the C2 motif, we performed rescue experiments by co-injecting different combinations of MOs with capped *Nvmef2-II* mRNA. Injection of MOex9 together with wild-type *Nvmef2-II* (*Nvmef2-IIwt*) mRNA resulted in the development of normal primary polyps by day 6 in

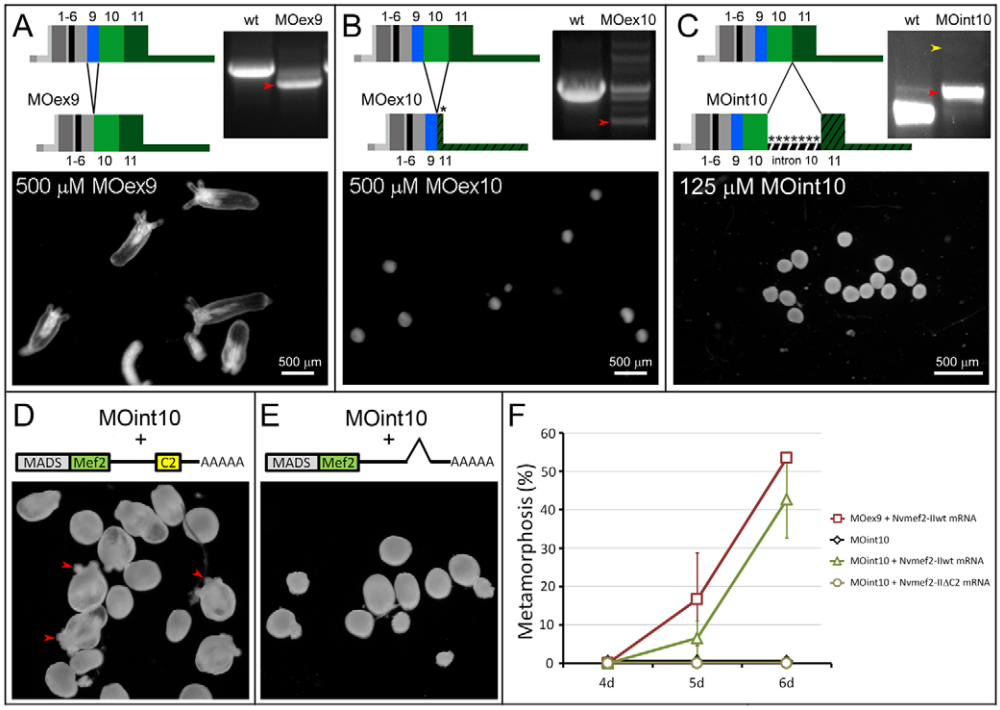

Fig. 3. Exons 10 and 11 encode a domain that is crucial for Nvmef2 function in the endoderm. (**A-C**) A scheme of action, the RT-PCR result and the phenotype (showing concentrations injected) of 8-day-old morphants are shown for each splice MO. (A) MOex9 causes deletion of exon 9, resulting in a lower band on the RT-PCR gel (arrowhead). This, however, does not affect the normal development of the embryos into primary polyps. (B) MOex10 causes deletion of exon 10 and a frame shift that generates a premature stop codon in exon 11 (asterisk). The mis-splicing is not very efficient. Multiple mis-spliced products are produced owing to cryptic splice cites. The 'correctly' mis-spliced product is indicated (arrowhead). The embryos have a severe endodermal phenotype similar to that shown in Fig. 2A. (C) MOint10 causes the inclusion of an intron 10 with multiple stop codons (asterisks) into the mature transcript. The mis-splicing is very efficient, but produces a shorter product (red arrowhead) than expected (yellow arrowhead) owing to the presence of the cryptic splice donor and acceptor within the intron. The phenotype is the same as for MOex10. (**D-F**) The C2 domain is essential for Nvmef2 function in the endoderm. The morphants shown in D,E are 6 days old. The structure of the injected *Nvmef2* mRNA, with the position of the encoded conserved protein domains indicated by boxes, is shown. (D) Co-injection of MOint10 together with *Nvmef2-IIwt* mRNA rescues the phenotype caused by the MO and results in the development of normal primary polyps in 42.7% of cases (arrowheads indicate tentacle buds). (E) No rescue is observed when MOint10 is co-injected together with *Nvmef2-IIΔC2*. (F) Average metamorphosis rate (percentage of primary polyps among the surviving embryos) of embryos co-injected with different combinations of *Nvmef2-II* mRNA and splice MOs. Four MO-RNA combinations (n=100-135 for each combination) were injected in three independent experiments. The large s.d. results from the variable speed of development of different batches of eggs. The values for MOint10 injected without mRNA (black curve) were manually set from 0% to 0.6% for visibility.

53.5% of cases (Fig. 3F; supplementary material Fig. S6A), showing that co-injection of *Nvmef2-IIwt* mRNA with a control MO does not perturb normal development. Co-injection of MOint10 together with *Nvmef2-IIwt* mRNA rescued the MOint10 phenotype (Fig. 3D,F; supplementary material Fig. S6C) and resulted in the development of normal primary polyps in 42.7% of cases by day 6. Strikingly, *Nvmef2-IIΔC2* mRNA, which lacks the C2 domain, had no rescue effect when co-injected with MOint10 (Fig. 3E,F) and the morphants were indistinguishable from those injected with MOint10 alone (supplementary material Fig. S6B,D). This allows us to conclude that the effect of the MO is specific and that both the conserved C2 domain encoded by exon 10 and the amino acids encoded by exon 11 are required for the proper function of Nvmef2 in endoderm development.

In *Nvmef2* morphants the endoderm forms but then loses integrity

Since the strongest phenotypic effect is seen in the endoderm, we asked whether it is gastrulation itself or the subsequent differentiation of the endoderm that is affected by *Nvmef2* knockdown. The zygotes injected with 500 μM MOex10 underwent normal gastrulation (Fig. 4A,D), but by day 2 the endodermal layer began to lose integrity and the archenteron filled with cells, whereas in controls the endoderm formed a columnar epithelium (compare Fig. 4B,C with 4E,F). The same effect was observed when zygotes were injected with MOint10 at 125 μM (data not shown). We conclude that endodermal *Nvmef2* is required for the maintenance of the endodermal layer and its proper differentiation.

We then tested whether the morphological changes in the embryo correlated with changes in cell proliferation. We assayed the morphant and control embryos for the number of cells passing through S phase of the cell cycle. The MOex9 and MOex10 morphants did not show significant differences in the S-phase index (the percentage of nuclei incorporating EdU) of their ectodermal cells as compared with uninjected controls (Mann-Whitney U-test for 2 day planula: P≤0.70, MOex10 versus uninjected; P≤0.34, MOex10 versus MOex9; P≤0.13, MOex9 versus uninjected; MOex10, n=6; MOex9, n=9; uninjected, n=8). However, very few endodermal cells of the MOex10 morphants

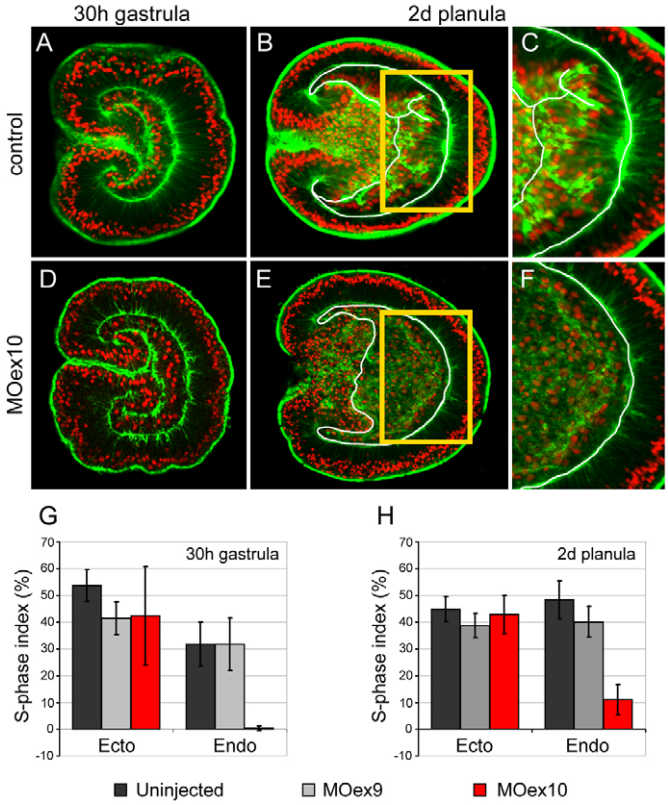

Fig. 4. Gastrulation and early planula development in control and morphant *Nematostella* embryos. (**A-C**) Phalloidin staining (green) of control 30-hour gastrula (A) and 2-day-old planula (B). Nuclei are counterstained with TO-PRO3 (red). The endoderm is outlined (white line). The area boxed in B is shown at higher magnification in C. The endodermal epithelium is well developed. (**D-F**) Phalloidin staining of morphant 30-hour gastrula (D) and 2-day-old planula (E). The area boxed in E is shown at higher magnification in F. The endoderm forms, but by day 2 becomes loose and starts to disintegrate. (**G**,**H**) S-phase index of uninjected embryos and morphant embryos injected with MOex9, which does not cause a phenotype, and MOex10, which causes a strong phenotype, in (G) 30-hour gastrula and (H) 2-day planula. Whereas the S-phase index in the ectoderm is similar in both types of morphants and in the uninjected controls, it is strongly reduced in the endoderm of MOex10 morphants. Bars indicate s.d.

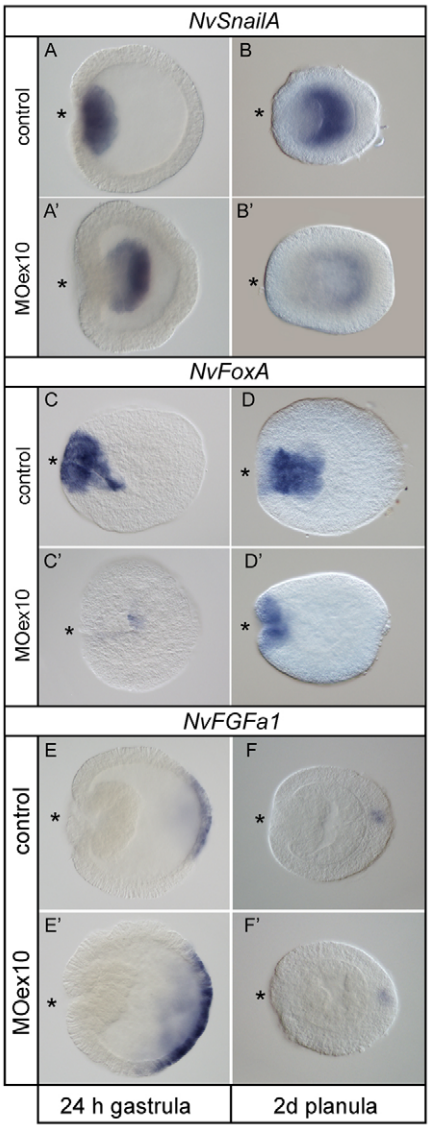

Fig. 5. Marker gene expression in control and MOex10-injected gastrulae and 2-day planulae. (**A-B'**) *NvSnailA* expression is normal in MOex10 morphant gastrulae (A,A′) and becomes weaker in 2-day planulae (B,B′). (**C-D'**) *NvFoxA* expression is delayed in morphant gastrulae (C,C′) and reduced to a superficial domain in 2-day planulae (D,D′). (**E-F'**) *NvFGFa1* expression retains the normal domain in the morphant but is slightly less intense than in the control. The size of the expression domain in the gastrulae varies in both controls and morphants, and hence the expansion of *NvFGFa1* (F′) cannot be attributed to the action of the MO. Asterisks indicate mouth position.

continued to replicate their DNA after gastrulation was complete (Fig. 4G), and in the 2-day planulae the S-phase index of the endodermal cells remained significantly lower ($P \leq 2.21 \times 10^{-7}$, MOex10 versus uninjected; $P \leq 2.16 \times 10^{-6}$, MOex10 versus MOex9; $P \leq 0.17$, MOex9 versus uninjected) than in the controls (Fig. 4H). The reduction in the S-phase index is reflected in the decreased number of endodermal cells in the 2-day MOex10 morphant planulae (supplementary material Fig. S7). Apoptosis does not appear to play a role in this, as no TUNEL-positive nuclei could be identified in 30- to 72-hour-old MOex10 morphants, i.e. during the time when the change in cell proliferation takes place (supplementary material Fig. S8).

To gain further insight into the effect of *Nvmef2* knockdown in the endoderm, we analysed the expression of three marker genes (Fig. 5; supplementary material Fig. S9A-C). As MOex10 and MOint10 showed the same phenotype for all genes examined, we will refer to the MOex10 phenotype. The early expression of the pan-endodermal marker *NvSnailA* (Fritzenwanker et al., 2004; Martindale et al., 2004) was unaffected but faded out gradually in the MOex10 morphants after completion of gastrulation (Fig. 5A-B′). This suggests that the endodermal *Nvmef2* splice variants have no effect on the initiation of *NvSnailA* expression but are necessary for its maintenance. The onset of expression of the pharyngeal marker *NvFoxA* (Fig. 5C-D′) (Martindale et al., 2004; Fritzenwanker et al., 2004) was delayed in comparison to the control (Fig. 5C,C′). At the 2-day planula stage, *NvFoxA* expression was detectable around the mouth (Fig. 5D,D′) but did not extend inside, indicating that the pharynx was not forming properly. Expression of the aboral ectodermal marker *NvFGFa1*

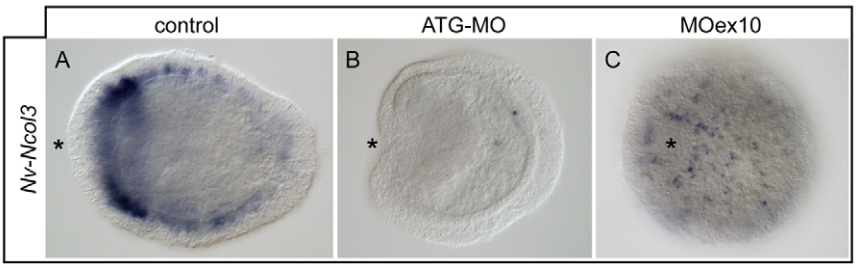

Fig. 6. Expression of the nematocyte marker gene *Nv-Ncol3* in 4-day-old *Nematostella* embryos. (**A**) control, (**B**) ATG-MO morphant and (**C**) surface view of the MOex10 morphant. *Nv-Ncol3* is expressed in ectodermal nematocytes in the control and MOex10 morphant, but not in the ATG-MO morphant. Asterisks indicate mouth position.

(Fig. 5E-F′) (Rentzsch et al., 2008) was, albeit slightly weaker at later stages of development, largely unaffected in the MOex10 morphants in terms of its expression domain, suggesting that the endodermally expressed *Nvmef2* splice variants have no effect on the patterning of the aboral ectoderm. Injection of the ATG-MO had very similar effects on the expression of *NvFoxA* and *NvSnailA* as the two endodermal splice MOs (supplementary material Fig. S9D,E and Fig. S10A-D′). However, *NvFGFa1* expression showed a significant enlargement of the aboral expression domain as well as ectopic expression at the oral end of the planula in ATG-MO morphant embryos. Moreover, in some cases, *NvFGFa1* was expressed throughout the ectoderm of the embryo (supplementary material Fig. S9F and Fig. S10E-F5). Since the ATG-MO affects the translation of all *Nvmef2* splice variants, this is likely to be an effect of the ectodermal splice variants.

Predicted Mef2 binding sites are not essential for *MyHC1::mCherry* transgene expression

In triploblasts, one of the most obvious functions of Mef2 is in the regulation of muscle differentiation. In morphant *Nematostella* lacking functional Nvmef2 protein, the retractor muscles do not form because endoderm development is impaired. However, the effect of the *Nvmef2* MOs manifests itself before the muscles start to form. We tested whether one of the characteristic targets of the Mef2 proteins in triploblasts, *MyHC1*, is under the direct regulation of Nvmef2. The *Nematostella MyHC1* gene is specifically expressed in retractor muscles (Renfer et al., 2010). A 1.6 kb regulatory fragment of *MyHC1*, which reproduces the normal expression pattern of *MyHC1* in a transgenesis assay (Renfer et al., 2010), contains three binding sites (predicted with high probability) for MADS box transcription factors: two Mef2 binding sites and one SQUA/Agamous binding site. However, polyps carrying an *MyHCΔMef::mCherry* transgene in which these three sites were mutated still expressed the mCherry reporter in the retractor muscles (supplementary material Fig. S11), suggesting that Nvmef2 binding to these sites is not essential for the expression of *MyHC1*. Further research will be required to reveal to what extent muscle development in *Nematostella* relies on regulation by Nvmef2.

ATG-MO, but not the endodermal splice morpholinos, affects neuron and nematocyte differentiation in the ectoderm

Because it has been proposed that *Nvmef2* is expressed in putative neuron or nematocyte precursors in the ectoderm (Martindale et al., 2004), we addressed the ectodermal function of *Nvmef2*. Unfortunately, producing specific MOs against the individual exon 7-containing splice variants is not technically possible, as this would require simultaneous blocking of four splice acceptor sites. Nevertheless, the effects of the ATG-MO and the endodermal splice MO on neuron and nematocyte differentiation can be compared using neuron and nematocyte markers. Whereas ATG-MO and MOex10 had very similar effects on the differentiation of FMRF amide-positive neurons (data not shown), a very clear difference in their effects on nematocyte differentiation was observed. In situ hybridisation of 4-day-old control and morphant planulae with a probe against the *N. vectensis* minicollagen gene *Nv-Ncol3*, which encodes a structural protein in the nematocyst (David et al., 2008), as well as TEM and histological analyses of 8-day-old morphant embryos, revealed that the ATG-MO morphants lack nematocytes in the ectoderm, whereas in MOex10 morphants the nematocytes are still present (Fig. 6A-D; supplementary material Fig. S4F-H and Fig. S9G). This suggests that only the ectodermally expressed, but not the endodermally expressed, *Nvmef2* splice variants are involved in the differentiation of nematocytes.

DISCUSSION

Alternative splicing considerably amplifies the size of the proteome encoded by a genome, and, where alternative splicing is developmentally regulated, the variants are thought to have distinct functions. In humans, up to 90% of all genes are thought to have alternative splice variants (Keren et al., 2010), which is considerably more than in *Drosophila*, *Caenorhabditis* and *Ciona* (Kim et al., 2007). Although the role of alternative splicing is extensively studied in *Drosophila* and vertebrates, very little is known about alternative splicing in lower Eumetazoa. Recently, the first report that alternative splice variants of the *Nematogalectin* gene are differentially expressed in different nematocyte types in *Hydra* was published (Hwang et al., 2010). Here, we demonstrate that alternative splice isoforms of an important developmental transcription factor, *Nvmef2*, have distinct expression domains and developmental functions in the sea anemone *N. vectensis*.

Similar to *NvMef2*, *Mef2* pro-mRNAs of flies and mammals are alternatively spliced (Martin et al., 1994; Gunthorpe et al., 1999; Zhu and Gulick, 2004; Zhu et al., 2005). Whereas the splice sites in the MADS and Mef2 domains are conserved between Cnidaria and Bilateria, the sequence coding for the C-terminal region, where the alternative splicing occurs, is too diverged to assess conservation of the splice cites. The two major classes of alternative *Nvmef2* splice variants differ in their expression pattern and in the size of the resulting proteins: the endodermally expressed variants are similar in size to the vertebrate Mef2 variants, whereas the ectodermal variants are shorter, lacking a

significant part of the transactivation domain. The molecular consequences of these differences in protein structure remain to be investigated.

Our results allow us to reconstruct the domain composition of the ancestral eumetazoan Mef2 protein. Besides the highly conserved N-terminal MADS and Mef2 domains, it contained two conserved motifs in the transactivation domain: the C1 domain and the C2 domain. The muscle-specific form of the C1 domain, encoded in vertebrates by exon 3α2, appears to be the only one present in *Nematostella* and other invertebrates (i.e. the ecdysozoan *Drosophila melanogaster* and lophotrochozoan *Lottia gigantea*) and in the basal chordate *Branchiostoma floridae*. Thus, the second variant of C1 (exon 3α1) and the alternative splicing of exons 3α1 and 3α2, as well as the alternatively spliced exons encoding the β-domains, appear to be vertebrate-specific innovations. The γ-domain has probably evolved at the base of Bilateria, as a very similar motif can be found in the transactivation domain of Mef2 in both *Drosophila melanogaster* and *Branchiostoma floridae*, but in these organisms it is not encoded by a specific alternatively spliced exon. This suggests that alternative splicing of cnidarian and bilaterian *Mef2* has either evolved independently or that the ancient exons of the transactivation domain have evolved beyond recognition.

In vertebrates, some of the different *Mef2* splice variants are expressed in different tissues. However, the expression of the different splice variants is mostly overlapping, and there might be some redundancy in function. Alternative splicing leads to the presence or absence of the so-called α-, β- and γ-domains, which affect protein function as a transcriptional activator or can even change it into a repressor (Martin et al., 1994; Zhu and Gulick, 2004; Zhu et al., 2005). An extra level of transcriptional, and possibly translational, regulation of Mef2A is conveyed by the use of two alternative promoters autoregulated by Mef2A protein and by the generation of several variants of the 5′ UTR by alternative splicing of the non-coding exons (Ramachandran et al., 2008). The situation in *Drosophila* is probably different in that it is not the particular splice isoforms but the amount of the protein that defines the identity of the differentiating cells (Gunthorpe et al., 1999). More recently, it has been shown that different levels of Mef2 activity are required for the regulation of the different Mef2 targets in *Drosophila* (Elgar et al., 2008).

In *Nematostella*, different *Nvmef2* splice variants are expressed in different cell types. Our data support the view (Martindale et al., 2004) that ectodermally expressed *Nvmef2* is either directly or indirectly involved in the regulation of the nematocyte and probably also in neuron differentiation. We also found that, in the endoderm, *Nvmef2* has another function. The earliest effect of *Nvmef2* knockdown is the arrest of cell proliferation in the endoderm after gastrulation. The subsequent endoderm differentiation is also affected by blocking *Nvmef2* translation and by improper splicing of the endodermally expressed splice variants. By contrast, splice MOs directed against the endodermally expressed *Nvmef2* variants have no effect on the development of ectodermal nematocytes. Surprisingly, despite the presence of the three predicted binding sites in the *MyHC1* promoter, so far we have found no evidence for Nvmef2 being a direct regulator of this key structural muscle differentiation gene in *Nematostella*, although it is a known target for Mef2 regulation in flies and mammals. Further experiments on other structural muscle genes are required to determine whether the role of Mef2 as a key muscle determinant evolved only in Bilateria.

Usually, evolutionary sequence conservation is a good indicator of the functional relevance of a protein domain. Our MO-mediated knockdown experiments revealed that exon 11 is crucial for the function of the endodermal splice variants; however, the amino acid sequence encoded by exon 11 is not conserved. On the contrary, the conserved C2 domain is encoded by exon 10. We hypothesized that both exon 10 and exon 11 are required for the function of endodermally expressed *Nvmef2*. This view is supported by the deletion study of Janson et al. (Janson et al., 2001), who showed that direct coupling of the region encompassing amino acids 312-367 of human MEF2C (which contains the C-terminal half of the C2 domain) to the MADS and Mef2 domains is sufficient to produce a functional transcriptional activator, whereas proteins lacking amino acids 312-350 are very weak activators. In line with a crucial role for this conserved motif in Nvmef2 function in the endoderm, we found that only the form of *Nvmef2* mRNA that contains the sequence encoding the C2 domain could rescue the severe phenotype caused by MOint10, whereas a protein lacking this domain was unable to rescue the phenotype. Thus, our experiments reveal a conserved motif in specific splice variants that is crucial for endoderm differentiation in the sea anemone. In vertebrates, the sequence encoding the C2 domain is split between two constitutive exons. Further biochemical analyses are required to understand the function of this domain.

Our results have demonstrated that *Nvmef2* is one of the key players driving post-gastrulation development. Two striking features of the development of *Nvmef2* morphants are; (1) their endoderm forms normally during gastrulation but then loses integrity and the proliferation of the endodermal cells becomes suppressed; and (2) the pharynx fails to differentiate during planula development. The latter might be due to the lack of an inducing signal from the endoderm. A genome-wide analysis of Nvmef2 target genes will be necessary to explain the morphant phenotype.

The evolution of the mesoderm is one of the key developmental questions that can be addressed by comparing cnidarians with triploblasts. Surprisingly, diploblastic cnidarians have most of the important mesodermal determinants. The expression of these genes at the blastopore or in the endoderm of *Nematostella* argues for the common evolutionary origin of the endoderm and the mesoderm in triploblasts (Martindale et al., 2004; Technau and Scholz, 2003). Evidently, the presence of certain conserved transcription factors is not sufficient to induce a mesoderm, suggesting that the function of the individual genes and their gene regulatory network must have evolved. A functional diversification might be conveyed by novel cis-regulatory elements, by the addition of new protein-protein interfaces, or by alternative splicing combined with differential expression. The latter is thought to have played a major role in the diversification of gene function in vertebrates. Although a lower complexity of gene function might be expected in cnidarians on the basis of their simple morphology, our data show that, at least for *Mef2*, the involvement of alternative splice variants in the specification of neural cell types and the endomesoderm predates the cnidarian-bilaterian split.

Acknowledgements

We thank Michaela Schwaiger, Johannes Schinko and Patrick Steinmetz for critically reading the manuscript; Irene Lichtscheidl for confocal microscope facility support; Manuel Irimia (University of Barcelona) for help with splice site analysis; Anna Nyhaug and Trygve Knagg (Molecular Imaging Centre, University of Bergen) for help with transmission and scanning electron microscopy; Manfred Walzl and Stefan Jahnel for preparing semi-thin sections; and the staff of the animal facility.

Funding
G.G. was a recipient of the Marie Curie Incoming International Fellowship. This work was supported by grants from the Research Council of Norway (NFR); and the European Initial Training Network (EU-ITN) EVONET to U.T.

Competing interests statement
The authors declare no competing financial interests.

Supplementary material
Supplementary material available online at
http://dev.biologists.org/lookup/suppl/doi:10.1242/dev.068122/-/DC1

References
Ananieva, O., Macdonald, A., Wang, X., McCoy, C. E., McIlrath, J., Tournier, C. and Arthur, J. S. (2008). ERK5 regulation in naive T-cell activation and survival. *Eur. J. Immunol.* **38**, 2534-2547.
Arnold, M. A., Kim, Y., Czubryt, M. P., Phan, D., McAnally, J., Qi, X., Shelton, J. M., Richardson, J. A., Bassel-Duby, R. and Olson, E. N. (2007). MEF2C transcription factor controls chondrocyte hypertrophy and bone development. *Dev. Cell* **12**, 377-389.
Bachinski, L. L., Sirito, M., Bohme, M., Baggerly, K. A., Udd, B. and Krahe, R. (2010). Altered MEF2 isoforms in myotonic dystrophy and other neuromuscular disorders. *Muscle Nerve* **42**, 856-863.
Black, B. L., Lu, J. and Olson, E. N. (1997). The MEF2A 3′ untranslated region functions as a cis-acting translational repressor. *Mol. Cell. Biol.* **17**, 2756-2763.
Blanchard, F. J., Collins, B., Cyran, S. A., Hancock, D. H., Taylor, M. V. and Blau, J. (2010). The transcription factor Mef2 is required for normal circadian behavior in Drosophila. *J. Neurosci.* **30**, 5855-5865.
David, C. N., Ozbek, S., Adamczyk, P., Meier, S., Pauly, B., Chapman, J., Hwang, J. S., Gojobori, T. and Holstein, T. W. (2008). Evolution of complex structures: minicollagens shape the cnidarian nematocyst. *Trends Genet.* **24**, 431-438.
Elgar, S. J., Han, J. and Taylor, M. V. (2008). mef2 activity levels differentially affect gene expression during Drosophila muscle development. *Proc. Natl. Acad. Sci. USA* **105**, 918-923.
Farris, S. M., Robinson, G. E., Davis, R. L. and Fahrbach, S. E. (1999). Larval and pupal development of the mushroom bodies in the honey bee, Apis mellifera. *J. Comp. Neurol.* **414**, 97-113.
Flavell, S. W., Cowan, C. W., Kim, T. K., Greer, P. L., Lin, Y., Paradis, S., Griffith, E. C., Hu, L. S., Chen, C. and Greenberg, M. E. (2006). Activity-dependent regulation of MEF2 transcription factors suppresses excitatory synapse number. *Science* **311**, 1008-1012.
Flavell, S. W., Kim, T. K., Gray, J. M., Harmin, D. A., Hemberg, M., Hong, E. J., Markenscoff-Papadimitriou, E., Bear, D. M. and Greenberg, M. E. (2008). Genome-wide analysis of MEF2 transcriptional program reveals synaptic target genes and neuronal activity-dependent polyadenylation site selection. *Neuron* **60**, 1022-1038.
Fritzenwanker, J. H. and Technau, U. (2002). Induction of gametogenesis in the basal cnidarian Nematostella vectensis (Anthozoa). *Dev. Genes Evol.* **212**, 99-103.
Fritzenwanker, J. H., Saina, M. and Technau, U. (2004). Analysis of forkhead and snail expression reveals epithelial-mesenchymal transitions during embryonic and larval development of Nematostella vectensis. *Dev. Biol.* **275**, 389-402.
Fritzenwanker, J. H., Genikhovich, G., Kraus, Y. and Technau, U. (2007). Early development and axis specification in the sea anemone Nematostella vectensis. *Dev. Biol.* **310**, 264-279.
Genikhovich, G. and Technau, U. (2009a). Induction of spawning in the starlet sea anemone Nematostella vectensis, in vitro fertilization of gametes, and dejellying of zygotes. *CSH protocols 2009*, pdb prot5281.
Genikhovich, G. and Technau, U. (2009b). In situ hybridization of starlet sea anemone (Nematostella vectensis) embryos, larvae, and polyps. *CSH protocols 2009*, pdb prot5282.
Genikhovich, G. and Technau, U. (2009c). Anti-acetylated tubulin antibody staining and phalloidin staining in the starlet sea anemone Nematostella vectensis. *CSH protocols 2009*, pdb prot5283.
Gunthorpe, D., Beatty, K. E. and Taylor, M. V. (1999). Different levels, but not different isoforms, of the Drosophila transcription factor DMEF2 affect distinct aspects of muscle differentiation. *Dev. Biol.* **215**, 130-145.
Hakim, N. H., Kounishi, T., Alam, A. H., Tsukahara, T. and Suzuki, H. (2010). Alternative splicing of Mef2c promoted by Fox-1 during neural differentiation in P19 cells. *Genes Cells* **15**, 255-267.
Hwang, J. S., Takaku, Y., Momose, T., Adamczyk, P., Ozbek, S., Ikeo, K., Khalturin, K., Hemmrich, G., Bosch, T. C. G., Holstein, T. W. et al. (2010). Nematogalectin, a nematocyst protein with GlyXY and galectin domains, demonstrates nematocyte-specific alternative splicing in Hydra. *Proc. Natl. Acad. Sci. USA* **107**, 18539-18544.
Janson, C. G., Chen, Y., Li, Y. and Leifer, D. (2001). Functional regulatory regions of human transcription factor MEF2C. *Mol. Brain Res.* **97**, 70-82.
Keren, H., Lev-Maor, G. and Ast, G. (2010). Alternative splicing and evolution: diversification, exon definition and function. *Nat. Rev. Genet.* **11**, 345-355.
Kim, E., Magen, A. and Ast, G. (2007). Different levels of alternative splicing among eukaryotes. *Nucleic Acids Res.* **35**, 125-131.
Lenhard, B., Sandelin, A., Mendoza, L., Engstrom, P., Jareborg, N. and Wasserman, W. W. (2003). Identification of conserved regulatory elements by comparative genome analysis. *J. Biol.* **2**, 13.
Martin, J. F., Miano, J. M., Hustad, C. M., Copeland, N. G., Jenkins, N. A. and Olson, E. N. (1994). A Mef2 gene that generates a muscle-specific isoform via alternative mRNA splicing. *Mol. Cell. Biol.* **14**, 1647-1656.
Martindale, M. Q., Pang, K. and Finnerty, J. R. (2004). Investigating the origins of triploblasty: 'mesodermal' gene expression in a diploblastic animal, the sea anemone Nematostella vectensis (phylum, Cnidaria; class, Anthozoa). *Development* **131**, 2463-2474.
Potthoff, M. J. and Olson, E. N. (2007). MEF2: a central regulator of diverse developmental programs. *Development* **134**, 4131-4140.
Ramachandran, B., Yu, G., Li, S., Zhu, B. and Gulick, T. (2008). Myocyte enhancer factor 2A is transcriptionally autoregulated. *J. Biol. Chem.* **283**, 10318-10329.
Renfer, E., Amon-Hassenzahl, A., Steinmetz, P. R. and Technau, U. (2010). A muscle-specific transgenic reporter line of the sea anemone, Nematostella vectensis. *Proc. Natl. Acad. Sci. USA* **107**, 104-108.
Rentzsch, F., Fritzenwanker, J. H., Scholz, C. B. and Technau, U. (2008). FGF signalling controls formation of the apical sensory organ in the cnidarian Nematostella vectensis. *Development* **135**, 1761-1769.
Sandmann, T., Jensen, L. J., Jakobsen, J. S., Karzynski, M. M., Eichenlaub, M. P., Bork, P. and Furlong, E. E. (2006). A temporal map of transcription factor activity: mef2 directly regulates target genes at all stages of muscle development. *Dev. Cell* **10**, 797-807.
Sandmann, T., Girardot, C., Brehme, M., Tongprasit, W., Stolc, V. and Furlong, E. E. (2007). A core transcriptional network for early mesoderm development in Drosophila melanogaster. *Genes Dev.* **21**, 436-449.
Schulz, R. A., Chromey, C., Lu, M. F., Zhao, B. and Olson, E. N. (1996). Expression of the D-MEF2 transcription in the Drosophila brain suggests a role in neuronal cell differentiation. *Oncogene* **12**, 1827-1831.
Spring, J., Yanze, N., Josch, C., Middel, A. M., Winninger, B. and Schmid, V. (2002). Conservation of Brachyury, Mef2, and Snail in the myogenic lineage of jellyfish: a connection to the mesoderm of bilateria. *Dev. Biol.* **244**, 372-384.
Technau, U. and Scholz, C. B. (2003). Origin and evolution of endoderm and mesoderm. *Int. J. Dev. Biol.* **47**, 531-539.
Technau, U., Rudd, S., Maxwell, P., Gordon, P. M., Saina, M., Grasso, L. C., Hayward, D. C., Sensen, C. W., Saint, R., Holstein, T. W. et al. (2005). Maintenance of ancestral complexity and non-metazoan genes in two basal cnidarians. *Trends Genet.* **21**, 633-639.
Verzi, M. P., Agarwal, P., Brown, C., McCulley, D. J., Schwarz, J. J. and Black, B. L. (2007). The transcription factor MEF2C is required for craniofacial development. *Dev. Cell* **12**, 645-652.
Wang, D. Z., Valdez, M. R., McAnally, J., Richardson, J. and Olson, E. N. (2001). The Mef2c gene is a direct transcriptional target of myogenic bHLH and MEF2 proteins during skeletal muscle development. *Development* **128**, 4623-4633.
Wang, X., She, H. and Mao, Z. (2009). Phosphorylation of neuronal survival factor MEF2D by glycogen synthase kinase 3beta in neuronal apoptosis. *J. Biol. Chem.* **284**, 32619-32626.
Watanabe, H., Hoang, V. T., Mattner, R. and Holstein, T. W. (2009). Immortality and the base of multicellular life: Lessons from cnidarian stem cells. *Semin. Cell Dev. Biol.* **20**, 1114-1125.
Yu, Y. T., Breitbart, R. E., Smoot, L. B., Lee, Y., Mahdavi, V. and Nadal-Ginard, B. (1992). Human myocyte-specific enhancer factor 2 comprises a group of tissue-restricted MADS box transcription factors. *Genes Dev.* **6**, 1783-1798.
Zhu, B. and Gulick, T. (2004). Phosphorylation and alternative pre-mRNA splicing converge to regulate myocyte enhancer factor 2C activity. *Mol. Cell. Biol.* **24**, 8264-8275.
Zhu, B., Ramachandran, B. and Gulick, T. (2005). Alternative pre-mRNA splicing governs expression of a conserved acidic transactivation domain in myocyte enhancer factor 2 factors of striated muscle and brain. *J. Biol. Chem.* **280**, 28749-28760.